NASTRAN CYCLIC SYMMETRY CAPABILITY

By R. H. MacNeal and R. L. Harder

The MacNeal-Schwendler Corp., Los Angeles

and J. B. Mason

NASA Goddard Space Flight Center

SUMMARY

The paper describes a recent development for NASTRAN which facilitates the analysis of structures made up of identical segments symmetrically arranged with respect to an axis. The key operation in the method is the transformation of the degrees of freedom for the structure into uncoupled *symmetrical components*, thereby greatly reducing the number of equations which are solved simultaneously. A further reduction occurs if each segment has a plane of reflective symmetry. The only required assumption is that the problem be linear. The capability, as developed, will be available in Level 16 of NASTRAN for static stress analysis, steady state heat transfer analysis, and vibration analysis.

The paper includes a discussion of the theory, a brief description of the data supplied by the user, and the results obtained for two example problems. The first problem concerns the acoustic modes of a long prismatic cavity imbedded in the propellant grain of a solid rocket motor. The second problem involves the deformations of a large space antenna. The latter example is the first application of the NASTRAN Cyclic Symmetry capability to a really large problem.

INTRODUCTION

Many structures, including pressure vessels, rotating machines, and antennas for space communications, are made up of virtually identical segments that are symmetrically arranged with respect to an axis. There are two types of cyclic symmetry as shown in Figures 1 and 2: *simple rotational symmetry*, in which the segments do not have planes of reflective symmetry and the boundaries between segments may be general doubly-curved surfaces, and *dihedral symmetry*, in which each segment has a plane of reflective symmetry and the boundaries between segments are planar. In both cases, it is most important for reasons of economy to be able to calculate the thermal and structural response by analyzing a subregion containing as few segments as possible.

Principles of reflective symmetry (which are not, in general, satisfied by cyclically symmetric bodies) can reduce the analysis region to one-fourth of the whole. Principles of cyclic symmetry, on the other hand, can reduce the

analysis region to a single segment in the case of dihedral symmetry and to a pair of segments in the case of simple rotational symmetry. Neither accuracy nor generality need be lost in the process, except that the treatment is limited to linear relationships between degrees of freedom.

Special procedures for the treatment of Cyclic Symmetry have recently been added to NASTRAN under the sponsorship of the Goddard Space Flight Center. The procedures will be available in Level 16 of NASTRAN. This paper includes a discussion of the theory, a description of the special input data, and the solutions of example problems. More complete information, including detailed descriptions of new functional modules and DMAP ALTERS for Rigid Formats 1 and 3, is contained in Ref. 1.

The use of cyclic symmetry will allow the analyst to model (i.e., make a NASTRAN Bulk Data Deck for) only one of the identical substructures. There will also be a large saving of computer time for most problems.

THEORY

Two types of cyclic symmetry are shown in Figures 1 and 2, where they are called *rotational* symmetry and *dihedral* symmetry. The latter term is borrowed from Herman Weyl who used it in his mathematical treatment of symmetry, Ref. 2. Note that dihedral symmetry is a special case of rotational symmetry. In both cases, the body is composed of identical segments, each of which obeys the same physical laws. The distortions (deflections or temperature changes) of the segments are not independent, but must satisfy compatibility at the boundaries between segments. Cyclic transforms will be defined, which are linear combinations of the distortions of the segments. The transformed equations of compatibility are such that the "transformed segments" are coupled singly or in pairs which can be solved *independently*. This feature results in a significant reduction of computational effort *beyond* the normal possibilities of substructure analysis.

In the theory given below, the form of the transformation is not derived, but just stated. The validity of the method is then demonstrated. A step-by-step inductive derivation of the transformation will be found in Ref. 3. The theory will be presented first for the more general but simpler case of rotational symmetry, after which the additional special features for dihedral symmetry will be introduced.

Theory for Rotational Symmetry

The total body consists of N identical segments, which are numbered consecutively from 1 to N. The user supplies a NASTRAN model for one segment. All other segments and their coordinate systems are rotated to equally-spaced positions about the polar axis. The boundaries must be *conformable*; i.e., when the segments are put together, the grid points and the displacement coordinate systems of adjacent segments must coincide. This is easiest to insure if a

cylindrical or spherical coordinate system is used, but such is not required. The user will also supply a paired list of grid points on the two boundaries of the segment where connections will be made. For static analysis the user may also supply a set of loads and/or enforced displacements for each of the N segments.

The two boundaries will be called sides 1 and 2. Side 2 of segment n is connected to side 1 of segment n+1, see Figure 1. Thus, the components of displacement satisfy

$$u_1^{n+1} = u_2^n \qquad n = 1, 2, \ldots, N \tag{1}$$

where the superscript refers to the segment index and the subscript refers to the side index. This applies to all degrees of freedom which are joined together. We also define $u^{n+1} = u^1$, so that Equation 1 will refer to all boundaries. Equation 1 is the equation of constraint between the physical segments.

The rotational transformation is given by

$$u^n = \bar{u}^o + \sum_{k=1}^{k_L} [\bar{u}^{kc} \cos(n-1)ka + \bar{u}^{ks} \sin(n-1)ka] + (-1)^{n-1} \bar{u}^{N/2} \tag{2}$$

$$a = 2\pi/N, \quad n = 1, 2, \ldots, N$$

where u^n *can be any component* of a displacement, force, stress, temperature, etc., in the n^{th} segment. The last term exists only when N is even. The summation limit $k_L = (n-1)/2$ if N is odd and $(N-2)/2$ if N is even. $\bar{u}^o$, $\bar{u}^{kc}$, $\bar{u}^{ks}$, and $\bar{u}^{N/2}$ are the transformed quantities which will be referred to as *symmetrical components*. They are given this designation by virtue of their similarity to the symmetrical components used by electrical engineers in their analysis of polyphase networks, Ref. 4. Note also the similarity of Equation 2 to a Fourier series decomposition, except that the number of terms is finite. On this account, Equation 2 could be called a finite Fourier transformation, Ref. 5.

Equation 2 can be displayed in the matrix form

$$[u] = [\bar{u}][T] \tag{3}$$

where $$[u] = [u^1, u^2, u^3, \ldots, u^N]$$

and $$[\bar{u}] = [\bar{u}^o, \bar{u}^{1c}, \bar{u}^{1s}, \bar{u}^{2c}, \bar{u}^{2s}, \ldots, \bar{u}^{N/2}]$$

Each element in the first row vector can represent all of the unknowns in one segment.

The expanded form of the transformation matrix is

$$[T] = \begin{bmatrix} 1 & 1 & 1 & \cdots & 1 \\ \hline 1 & \cos a & \cos 2a & \cdots & \cos (N-1)a \\ 0 & \sin a & \sin 2a & \cdots & \sin (N-1)a \\ \hline 1 & \cos 2a & \cos 4a & & \cos (N-1)2a \\ \vdots & \vdots & \vdots & & \vdots \\ 0 & \sin k_L a & \sin 2k_L a & \cdots & \sin (N-1)k_L a \\ \hline 1 & -1 & 1 & \cdots & -1 \end{bmatrix} \tag{4}$$

The last row exists only for even N. The transformation matrix, [T], has the property

$$[T]\,[T]^T = [D] = \begin{bmatrix} N & & & & & \\ & N/2 & & & & \\ & & N/2 & & & \\ & & & N/2 & & \\ & & & & \ddots & \\ & & & & & N \end{bmatrix} \tag{5}$$

i.e., the rows of [T] are orthogonal.

Since D is nonsingular,

$$[T][T]^T[D]^{-1} = [I] \tag{6}$$

Thus, $[T]^{-1} = [T]^T[D]^{-1}$ and

$$\lfloor \bar{u} \rfloor = \lfloor u \rfloor [T]^{-1} = \lfloor u \rfloor [T^T D^{-1}] \tag{7}$$

In summation form, Equation 7 becomes

$$\bar{u}^o = (1/N) \sum_{n=1}^{N} u^n \tag{8a}$$

$$\bar{u}^{kc} = (2/N) \sum_{n=1}^{N} u^n \cos(n-1)ka \tag{8b}$$

$$\bar{u}^{ks} = (2/N) \sum_{n=1}^{N} u^n \sin(n-1)ka \tag{8c}$$

$$\bar{u}^{N/2} = (1/N) \sum_{n=1}^{N} (-1)^{n-1} u^n \quad (N \text{ even only}) \tag{8d}$$

It should be noted that Equations 8 apply to applied loads and to internal forces as well as displacement components. The validity of the symmetrical components $\lfloor \bar{u} \rfloor$ to represent the motions of the system follows from the existence of $[T]^{-1}$. It remains only to show that they are useful. The equations of motion at points interior to the segments are linear (homogenous of degree 1) in displacements, forces, and temperatures; they are identical for all segments; and they are not coupled between segments.

Thus, the equations of motion (for example $[K]\{u\}^n = \{P\}^n$ in static analysis) can be additively combined using one of the sets of coefficients in Equation 8, thereby obtaining the equations of motion for one of the transformed variables which will have identically the same form (e.g., $[K]\{\bar{u}\}^{kc} = \{\bar{P}\}^{kc}$) as the equations of motion for one of the physical segments.

The equations of motion at points on the boundaries between segments are treated by employing the notion of a rigid constraint connecting adjacent points. To transform the compatibility equation of constraint (1), notice that

$$u_1^{n+1} = \bar{u}_1^o + \sum_{k=1}^{k_L} [\bar{u}_1^{kc} \cos nka + \bar{u}_1^{ks} \sin nka] + (-1)^n \bar{u}_1^{N/2} \qquad (9)$$

Using the identities cos nka = cos(n-1)ka·cos ka - sin(n-1)ka·sin ka and sin nka = sin(n-1)ka·cos ka + cos(n-1)ka·sin ka, Equation 9 may be written

$$u_1^{n+1} = \bar{u}_1^o + \sum_{k=1}^{k_L} \begin{bmatrix} (\bar{u}_1^{kc} \cos ka + \bar{u}_1^{ks} \sin ka)\cos(n-1)ka \\ +(-\bar{u}_1^{kc} \sin ka + \bar{u}_1^{ks} \cos ka)\sin(n-1)ka \end{bmatrix} - (-1)^{n-1} \bar{u}_1^{N/2} \qquad (10)$$

Comparing Equation 10 with Equation 2 evaluated at side 2 as required by Equation 1, and equating the coefficients of terms with the same dependence on n, we obtain

$$\bar{u}_1^o = \bar{u}_2^o \qquad (11a)$$

$$\left.\begin{aligned} \bar{u}_1^{kc} \cos ka + \bar{u}_1^{ks} \sin ka &= \bar{u}_2^{kc} \qquad (11b) \\ -\bar{u}_1^{kc} \sin ka + \bar{u}_1^{ks} \cos ka &= \bar{u}_2^{ks} \qquad (11c) \end{aligned}\right\} \quad k = 1, \cdots, k_L$$

$$-\bar{u}_1^{N/2} = \bar{u}_2^{N/2} \qquad (11d)$$

Equations 11 are the equations of constraint for the symmetrical components. The only symmetrical components coupled by the compatibility constraints are 1c and 1s, 2c and 2s, etc. Thus, there are several *uncoupled* models; the K=0 model contains the $\bar{u}^o$ degrees of freedom; the K = 1 model, the $\bar{u}^{1c}$ and $\bar{u}^{1s}$ degrees of freedom, etc.

There is a somewhat arbitrary choice regarding where to transform the variables in the NASTRAN analysis. NASTRAN structural analysis can start with a structure defined with single and multipoint constraints, applied loads, thermal fields, etc., and reduce the problem to the "analysis set," $\{u_a\}$, where

$$[K_{aa}]\{u_a\} = \{P_a\} \qquad (12)$$

The vector $\{u_a\}$ contains only independent degrees of freedom. The decision was made in developing the cyclic symmetry capability to first reduce each segment individually to the "analysis" degrees of freedom and then to transform the remaining freedoms to symmetrical components. This approach has several advantages, including elimination of the requirement to transform temperature vectors and single-point enforced displacements, because these quantities are first converted into equivalent loads. More importantly, if the "ØMIT" feature is used to remove internal degrees of freedom, it need only be applied to one segment. The ØMIT feature greatly reduces the number of degrees of freedom which must be transformed. The user specifies all constraints internal to the segments with standard NASTRAN data cards. If constraints (MPC, SPC, and/or ØMIT) are applied to degrees of freedom on the boundaries, they will take precedence over the intersegment compatibility constraints; i.e., an intersegment compatibility constraint will *not* be applied to any degree of freedom which is constrained in some other way. SUPØRT data cards are forbidden because they are intended to apply to overall rigid body motions and will not, therefore, be applied to each segment. In the case of static analysis, the analysis equations for the segments are

$$[K]\{u\}^n = \{P\}^n \qquad n = 1, 2, \ldots, N \tag{13}$$

The analysis equations for the symmetrical components, prior to applying the intersegment constraints, are

$$[K]\{\bar{u}\}^x = \{\bar{P}\}^x \qquad x = 0, 1c, 1s, 2c, \ldots, N/2 \tag{14}$$

where $\{\bar{P}\}^x$ is calculated using Equations 8. The matrix [K] is the same for Equations 13 and 14 and is the KAA stiffness matrix of NASTRAN for one segment.

We come now to the matter of applying the intersegment compatibility constraints. It is recognized that not all of the degrees of freedom in any transformed model can be independent, but it is easy to choose an independent set. We include in the independent set, $\{\bar{u}\}^K$, all points in the interior and on boundary 1 (for both $\bar{u}^{kc}$ and $\bar{u}^{ks}$, if they exist). The values of displacement components at points on boundary 2 can then be determined from Equations 11. The transformation to the new set of *independent* degrees of freedom is indicated by

$$\{\bar{u}\}^{kc} = [G_{ck}]\{\bar{u}\}^K \tag{15a}$$

$$\{\bar{u}\}^{ks} = [G_{sk}]\{\bar{u}\}^K \tag{15b}$$

where each row of $[G_{ck}]$ or $[G_{sk}]$ contains only a single nonzero term if it is

an interior or side 1 degree of freedom and either one or two nonzero terms if it is a degree of freedom on side 2. In arranging the order of terms in $\{\bar{u}\}^K$, the user can specify either that they be sequenced with all $\{\bar{u}\}^{kc}$ terms preceding all $\{\bar{u}\}^{ks}$ terms, or that they be sequenced with $\{\bar{u}\}^{kc}$ and $\{\bar{u}\}^{ks}$ grid points alternating. It should be emphasized that the kind of vectors used in transformation of Equations 3 and 15 are quite different. In Equation 3, there is one component (or column) for each segment; in Equation 15, there is one component (or row) for each degree of freedom in a segment.

Equation 15 is used to transform Equation 14 to the following set of equations which satisfy the intersegment compatibility conditions:

$$[\bar{k}]^K\{\bar{u}\}^K = \{\bar{p}\}^K \tag{16}$$

where

$$[\bar{k}]^K = [G_{ck}^T \; KG_{ck} + G_{sk}^T \; KG_{sk}] \tag{17}$$

and

$$\{\bar{p}\}^K = [G_{ck}^T]\{\bar{p}\}^{kc} + [G_{sk}^T]\{\bar{p}\}^{ks} \tag{18}$$

Because NASTRAN has sparse matrix routines of near optimum efficiency, the time for the calculations indicated in Equations 17 and 18 will not be appreciable. After solving Equation 16 by decomposition and substitution, the symmetrical component variables, $\{\bar{u}\}^{kc}$ and $\{\bar{u}\}^{ks}$, are found from Equations 15. The physical segment variables, $\{u\}^n$, are found from Equation 2. The $\{u\}^n$ are NASTRAN vectors of the analysis set. They may be expanded to $\{u_g\}$ size by recovering dependent quantities. Stresses in the physical segments are then obtained via the normal stress reduction procedures.

The user may take an alternate route if he knows the transformed values, $\{\bar{p}^{kc}\}$ and $\{\bar{p}^{ks}\}$, for the forcing functions (loads, enforced displacements, and temperatures). This will, for example, be the case in a stress analysis which follows a temperature analysis of the same structural model These data may be input directly to NASTRAN, which will convert them to the transformed load vectors, $\{\bar{p}\}^K$. Data reduction may also be performed on the transformed quantities to obtain the symmetrical components of stresses, etc.

A shortened approximate method for static analysis is available merely by setting

$$\{\bar{u}\}^K = 0 \tag{19}$$

for all K > KMAX. This is similar to truncating a Fourier series. The stiffness associated with larger K's (short azimuthal wave lengths) tends to be

large, so that these components of displacement tend to be small.

The cyclic symmetry method has also been coded for vibration analysis. The equation of motion in terms of independent degrees of freedom is

$$[\bar{K}^K - \omega^2 \bar{M}^K]\{\bar{u}\}^K = 0 \tag{20}$$

where $[\bar{M}]^K$ is derived by replacing [M] for [K] in Equation 17. The symmetrical components are recovered with Equation 15. No provision has been made to recover physical segment data in vibration analysis, because the physical interpretation of Equation 4 is straightforward. (Each row of [T] is a vector of the factors for each segment.) The available output data does, however, include the symmetrical components of dependent displacements, internal forces, and stresses.

Theory for Dihedral Symmetry

Dihedral symmetry refers to the case when each individual segment has a plane of reflective symmetry, see Figure 2. The segments are divided about their midplanes to obtain 2N substructures. The midplane of a segment is designated as side 2. The other boundary, which must also be planar, is called side 1. The two halves of the segment are called the right "R" and left "L" halves. The user prepares model information for one R half segment. He must also supply a list of points on side 1 and another list of points on side 2.

For the case of dihedral symmetry, the cyclic transformation described earlier is used in conjunction with reflective symmetry of the segments. The two transformations are commutable, so they may be done in either order. The reflective transform for a segment is

$$u^{n,R} = u^{n,S} + u^{n,A} \tag{21a}$$

$$u^{n,L} = u^{n,S} - u^{n,A} \tag{21b}$$

Here, the superscript n refers to the n^{th} segment, and R, L the right and left halves. S and A refer to the symmetric and antisymmetric reflective components.

In the R half segment, displacement components are referred to a right hand coordinate system and in the L half segment, displacement components are referred to a left hand coordinate system. The inverse reflective transform is

$$u^{n,S} = \tfrac{1}{2}(u^{n,R} + u^{n,L}) \tag{22a}$$

$$u^{n,A} = \tfrac{1}{2}(u^{n,R} - u^{n,L}) \tag{22b}$$

Reflective symmetry is seen to be very simple. The equations of motion at interior points of the S and A half-segment models are identical in form provided that unsymmetrical effects, such as Coriolis forces, are excluded.

The $u^{n,S}$ and $u^{n,A}$ components may be transformed as follows using rotational principles.

$$u^{n,x} = \bar{u}^{o,x} + \sum_{k=1}^{k_L} [\bar{u}^{kc,x} \cos(n-1)ka + \bar{u}^{ks,x} \sin(n-1)ka] + (-1)^{n-1} \bar{u}^{N/2,x} \tag{23}$$

where x may be either S (symmetric) or A(antisymmetric). The inverse transformation can be found by Equations 8 for both the symmetric and antisymmetric parts.

The constraints between the half segments are summarized in Table 1. The constraints shown apply between points joined together at the boundary planes. "Even components" include displacements parallel to the radial planes between segment halves, rotations about the axes normal to the planes, and temperatures in a thermal analysis. "Scalar points" in a structural analysis have arbitrarily been categorized as even components. "Odd components" include displacements normal to the radial planes and rotations about axes parallel to the planes. In Table 1 the constraint equations for the S and A half-segment model are obtained by substituting Equations 21 into the equations for the L and R half-segment model. The constraint equations for the dihedral transform model are obtained by substituting for $u^{n,x}$ and $u^{n+1,x}$ from Equation 23 and comparing terms with the same dependence on n. It can be seen in the table that the k = 0 and k = N/2 models are completely uncoupled. There is coupling between the kc,S and ks,A models and also between kc,A and ks,S models. These two sets of constraint equations are related and one can be found from the other by substituting $\bar{u}^{kc,S}$ for $\bar{u}^{ks,S}$ and $\bar{u}^{ks,A}$ for $-\bar{u}^{kc,A}$ in the constraint equations. With these substitutions, and noting that the equations of motion are identical at interior points, it is seen that we only need to analyze one coupled pair of symmetric and antisymmetric half segments with different load sets for the $(\bar{u}^{kc,S}, \bar{u}^{ks,A})$ case and the $(\bar{u}^{ks,S}, -\bar{u}^{kc,A})$ case.

As in the case of general rotational symmetry, a combined set of independent degrees of freedom is formed from the half models. The independent set $\{\bar{u}\}^k$ includes all interior points, the points on side 2 of each half segment

which are not constrained to zero, and new degrees of freedom, $\{\bar{u}_1\}^K$, on side 1 such that, for *even* components in the $(\bar{u}^{kc,S}, \bar{u}^{ks,A})$ case:

$$\bar{u}_1^{kc,S} = \cos\frac{k\pi}{N}\,\bar{u}_1^K \tag{24a}$$

$$\bar{u}_1^{ks,A} = \sin\frac{k\pi}{N}\,\bar{u}_1^K \tag{24b}$$

while for *odd* components:

$$\bar{u}_1^{kc,S} = -\sin\frac{k\pi}{N}\,\bar{u}_1^K \tag{25a}$$

$$\bar{u}_1^{ks,A} = \cos\frac{k\pi}{N}\,\bar{u}_1^K \tag{25b}$$

Equations 24 and 25 are equivalent to the constraints in the third column of Table 1. The transformation to the new set of independent freedoms may be expressed as

$$\{\bar{u}\}^{kc,S} = [G_{SK}]\{\bar{u}\}^K \tag{26a}$$

$$\{\bar{u}\}^{ks,A} = [G_{AK}]\{\bar{u}\}^K \tag{26b}$$

where each row of $[G_{SK}]$ or $[G_{AK}]$ contains at most a single nonzero term. The transformation matrices for the $(\bar{u}^{ks,S}, -\bar{u}^{kc,A})$ case are identical.

The final equation which is solved in static analysis is

$$[\bar{K}]^K\{\bar{u}\}^K = \{\bar{P}\}^K \tag{27}$$

where the stiffness matrix

$$[\bar{K}]^K = [G_{SK}^T\ K\ G_{SK} + G_{AK}^T\ K\ G_{AK}] \tag{28}$$

and the load vector is obtained by successive application of the inverse reflective symmetry transform, Equations 22, the inverse cyclic symmetry transform, Equations 8, and the final reduction to independent freedoms.

The form of the latter is, for the ($\bar{u}^{kc,S}$, $\bar{u}^{ks,A}$) case,

$$\{\bar{P}\}^K = [G_{SK}]^T\{\bar{P}\}^{kc,S} + [G_{AK}]^T\{\bar{P}\}^{ks,A} \tag{29}$$

and for the ($\bar{u}^{ks,S}$, $-u^{kc,A}$) case,

$$\{\bar{P}\}^K = [G_{SK}]^T\{\bar{P}\}^{ks,A} - [G_{AK}]^T\{\bar{P}\}^{kc,A} \tag{30}$$

The data reduction which follows the solution of Equation 27 in static analysis includes the application of the symmetry transformation to obtain $u^{n,R}$ and $u^{n,L}$, followed by the expansion to $\{u_g\}$ size for each half segment and the calculation of internal loads and stresses. Similar to the case of rotational symmetry, the data reduction for vibration analysis is limited to the recovery of eigenvectors, internal forces, and stresses for symmetrical component sets $\bar{u}^{kc,S}$ and $\bar{u}^{ks,A}$.

SUMMARY OF USER-SUPPLIED INFORMATION

The cyclic symmetry modification to NASTRAN allows the solution of structures with rotational or dihedral symmetry by modeling only one of the identical segments. Special Bulk Data cards and parameters are introduced to specify the method of joining the segments. Solutions are obtained by special DMAP ALTERS to Rigid Formats 1 and 3. In static analysis, input and output data for each individual segment are designated as separate subcases. The output includes, of course, the simultaneous effects of the loads on all segments. The constrained degrees of freedom and material properties must be the same for all segments. For static analysis, the loads, the values of enforced displacements, and the temperatures may vary from segment to segment. Separate loading conditions are also treated as subcases so that the total number of subcases equals the number of segments (or half segments) times the number of loading conditions.

The SPCD Bulk Data card (Figure 3) is useful for applying enforced boundary displacements (or temperatures). These values are requested by a load set; thus, if different displacements are specified on different segments (i.e., in different subcases), the requested SPC constraint set will not change. This must be done, since looping on constraint sets is not supported in cyclic symmetry analysis.

A Bulk Data card, CYJØIN (see Figure 4), is used to specify how the segments are to be connected. Existing MPC, SPC, and ØMIT constraints may be used within the segments. The SUPØRT card for free bodies is forbidden when cyclic symmetry is used, since *segment* free body modes do not necessarily imply

overall free body modes. Constraints between segments are applied automatically to the degrees of freedom at grid points specified on CYJØIN Bulk Data cards which are not otherwise constrained. Grid points are not allowed to be placed on the axis of symmetry.

The user must also define the following parameters by means of PARAM Bulk Data cards:

Parameter	Description
CYTYPE	Type of problem: RØT for rotational symmetry, DRL for dihedral symmetry using right and left halves, DSA for dihedral using symmetric and antisymmetric components.
N	Integer - The number of segments.
K	Integer - The value of the harmonic index, used only for eigenvalue analysis.
KMAX	Integer - The maximum value of K, used for static analysis. (Default is ALL)
CYCIØ	Integer - +1 for physical segment representation, -1 for cyclic transform representation for input and output of data. Static analysis, default = 1.
CYCSEQ	Integer - Used for method of sequencing the equations in the solution set. +1 for all cosine then all sine terms, -1 for alternating. Default = -1.
NLØAD	The number of loading conditions in static analysis. Default = 1.

MODIFICATIONS OF THE NASTRAN CODE

The NASTRAN modifications for cyclic symmetry include DMAP ALTERS to the Executive Control Deck and three new functional modules. The ALTERS and the details of the new functional modules are described in Reference 1. Briefly, the functions of the three modules are as follows:

The first module, called CPCYC, is a geometry processor acting on the CYJØIN data. It identifies and classifies the degrees of freedom involved in the boundary constraints.

The second module, called CYCT1, is used only in static analysis. It transforms excitation quantities (loads) from physical segment components to symmetrical components and it also transforms output displacements from symmetrical components to physical segment components. It is used for both types of symmetry (rotational and dihedral). All input and output quantities are "analysis-size" $\{u_a\}$ vectors.

The third module, called CYCT2, is used to transform load vectors and mass and stiffness matrices from symmetrical components to the solution set (see Equations 16, 17, 18, 28, 29, 30) and also to transform the results back to the symmetrical component sets.

ADVANTAGES

The NASTRAN cyclic symmetry capability will result in a large saving of user effort and computer time for most applications. The savings result from the following effects:

1. Grid point geometry and element data are prepared for only one segment in the case of rotational symmetry or one half segment in the case of dihedral symmetry.

2. The transformed equations are uncoupled, except within a given harmonic index, K, which reduces the order of the equations which must be solved simultaneously to 1/N or 2/N (where N is the number of segments or symmetrical half segments) times the order of the original system.

3. Solutions may be restricted to a partial range of the harmonic index, K, (e.g., to the lower harmonic orders) which results in a proportionate reduction in solution time. Some accuracy is thereby lost in the case of static analysis but not in vibration analysis.

4. In the case of static analysis, the ØMIT feature may be used to remove all degrees of freedom at internal grid points without any loss of accuracy. Since this reduction is applied to a single segment *prior* to the symmetry transformations, it can greatly reduce the amount of subsequent calculation.

It is instructive to compare the advantages of the NASTRAN cyclic symmetry capability with those offered by reflective symmetry and by conventional substructuring techniques. The savings offered by cyclic symmetry will always equal or exceed those provided by reflective symmetry except for possible differences due to time spent in transforming variables. For example, when an object has two planes of symmetry and two symmetrical segments (the minimum possible number in this case), the minimum region sizes are both equal to one half segment for the two methods. They are also equal when the object has four symmetrical segments. The advantages of cyclic symmetry for these cases are restricted to those offered by the ØMIT feature in static analysis and by a higher degree of input and output data organization. Any larger number of symmetrical segments increases the advantage of cyclic symmetry because the size of the fundamental region is smaller.

A method of conventional substructuring which recognizes identical substructures can also restrict the amount of grid point geometry and element data preparation to a single substructure and can use the ØMIT feature in the

same way as cyclic symmetry. The advantage which cyclic symmetry retains over conventional substructuring lies in its decomposition of degrees of freedom into uncoupled harmonic sets. This is an important advantage for eigenvalue extraction, but the advantage for static analysis is relatively small and depends in a complex manner on the number of segments and on the method of matrix decomposition.

In addition to the analysis of structures made up of a finite number of identical substructures, cyclic symmetry can also be used for purely axisymmetric structures. In this case the circumferential size of the analysis region is arbitrarily selected to be some small angle, for example, one degree. Grid points are then placed on the boundary surfaces but not in the interior of the region, and the region is filled with ordinary three-dimensional elements. The principal advantage of this procedure is that ordinary three-dimensional elements are used in place of *specialized* axisymmetric elements. In NASTRAN the number of available types and features for ordinary three-dimensional elements far exceeds those available for axisymmetric elements, so that cyclic symmetry immediately enlarges the analysis possibilities for axisymmetric structures. In particular, the rotational symmetry option can accommodate axisymmetric structures with nonorthotropic material properties, which the available axisymmetric procedures cannot. It is possible, in the long run, that cyclic symmetry will completely replace the relatively expensive NASTRAN axisymmetric capability. New input data cards modeled on existing axisymmetric data cards are needed to facilitate the use of cyclic symmetry for this purpose.

EXAMPLE PROBLEMS

Acoustic Vibrations of the Central Cavity in a Solid Rocket Motor

NASTRAN includes the ability to solve the acoustic wave equation which may be written in vector notation as

$$\nabla \cdot \frac{1}{\rho} \nabla P = \omega^2 \frac{1}{B} P \qquad (31)$$

where P is the pressure, ρ is the density, B is the bulk modulus, and ω is the frequency in radians per unit time. The theoretical development of finite fluid elements for solving problems with axisymmetric geometry is described in Section 16.3 of the NASTRAN Theoretical Manual, Reference 6. One of the products of that development, namely the family of CSLØT elements, can be used to solve the planar wave equation for a fluid disk of either constant or variable thickness, provided that there is no variation of pressure normal to the plane of the disk.

The CSLØT elements were used, in the present application, to model the prismatic central cavity of a typical solid rocket motor whose cross section is

shown in Figure 5. The cross-section has dihedral symmetry with seven segments (fourteen half segments). The axial length of the cavity is long compared to its diameter, and the problem of interest was the calculation of the lowest lateral vibration mode, i.e., the lowest mode exhibiting a pressure gradient across the diameter of the cavity. From the derivations described earlier in the paper, it is clear that the vibration modes of the cavity have distinct harmonic indices K; it is also clear, from physical reasoning, that K = 1 produces the lowest lateral mode. Thus, calculations were restricted to K = 1.

The finite element model for a single half segment is shown in Figure 6. It contains 71 grid points (with one degree of freedom per grid point), 39 triangular CSLØT3 elements and 29 quadrilateral CSLØT4 elements. A model based on reflective symmetry would have seven times as many finite elements. The mesh spacing is finer in the region where large pressure gradients are expected. Details of the modeling process for this problem are described in Reference 7. The frequency of the lowest lateral mode was calculated to be 17410 hertz. The distribution of radial velocities at lobe throats is indicated in Figure 5. The mode shape results produced by the computer are the symmetrical components, $\bar{u}^{1c,S}$ and $\bar{u}^{1s,A}$, for the pressures at grid points, and for the velocity components within elements. The formulas used to get physical components, obtained by combining Equations 21 and 23, are

Right Half Segments:

$$u^{n,R} = \bar{u}^{1c,S} \cos(n-1)a + \bar{u}^{1s,A} \sin(n-1)a \qquad (32a)$$

Left Half Segments:

$$u^{n,L} = \bar{u}^{1c,S} \cos(n-1)a - \bar{u}^{1s,A} \sin(n-1)a \qquad (32b)$$

Parabolic Reflector for the ATS-F Spacecraft

An artist's rendering of the deployed Lockheed 30-ft parabolic reflector on the ATS-F spacecraft is shown in Figure 7. The antenna is composed of 48 flexible aluminum ribs cantilevered symmetrically about a central hub at 7.5 degree increments. The reflective surface consists of a thin mesh woven from copper coated dacron yarn. When deployed, the mesh is under tension so as to remain taut during orbit.

The parabolic ribs have an "open-C" (i.e., semi-lenticular) cross section which tapers in both width and depth from the rib attachment at the central hub to the outer tip. This construction permits the ribs to be wrapped tightly around the hub in the stored configuration. As shown in Figure 8, integral stiffeners and varying diameter holes to accommodate deformations during storage are characteristic of the design. The nonisotropic mesh is formed by double strand radial and single strand circumferential yarn. Tests have shown that

Poisson's ratio is essentially zero for this material so that circumferential and radial yarns can be assumed to act independently.

It is clear from the shape of the ribs that the structure does not possess dihedral symmetry. It does, however, possess rotational symmetry and it was modeled by describing only one 7.5 degree segment. For the analysis the chosen segment had the rib centrally located with the mesh extending 3.75 degrees on either side. The rib was modeled using 745 grid points, i.e., 5 grid points through each section at 149 sections along the rib. 592 CQUAD2 elements, 60 CONRØD elements, and 300 CBAR elements were employed. The thicknesses of the quadrilaterals were adjusted to account for the holes, and the bars and rods were used to represent the integral stiffeners. 50 additional grid points were used to model the mesh, i.e., one mesh point on either side of the rib at each of 25 stations along the rib. The effects of the radial mesh strands were neglected in the analysis and only the circumferential strands were included. To represent the elastic stiffness of the mesh, 50 CRØD elements were attached circumferentially at the same 25 stations along the rib. 100 CELAS2 elements were employed at these stations to represent the radial and axial "string-stiffness" arising from the pre-tension in the mesh.

The ØMIT feature was utilized to reduce the original problem of nearly 4600 degrees of freedom to an analysis set containing 234 freedoms. This was accomplished by eliminating all freedoms on the rib except those at 14 points distributed along the edge next to the reflector. The 234 members of the analysis set consisted of 3 x 50 = 150 translational degrees of freedom at the boundary mesh points and 6 x 14 = 84 translational and rotational degrees of freedom along the rib. Model generation, Guyan reduction, and extraction of three eigenvalues using the inverse power method took about 30.0 minutes of CPU time on the Goddard Space Flight Center IBM 360/95 computer.

The computed frequencies for the three lowest axisymmetric (K = 0) modes and the lowest lateral (K = 1) mode are as follows:

K value	Freq. (hertz)
0	1.19 (test 1.17)
0	6.11
0	6.46
1	4.73

In the lowest K = 0 mode the tips of the ribs move collectively in the azimuthal direction. Its computed frequency compares well with the experimentally measured frequency.

REFERENCES

1. "NASTRAN Cyclic Symmetry User's Guide," The MacNeal-Schwendler Corporation Report EC-180, July 1972.

2. H. Weyl, "Symmetry," Lectures given at the Institute for Advanced Study, reprinted in The World of Mathematics, Simon and Schuster, New York, Vol. 1, pp 671-724, 1956.

3. R. H. MacNeal, "Principles of Rotor Dynamics," The MacNeal-Schwendler Corp. Report MSR-36, May 1973, Chapter 3.

4. C. E. Fortescue, "Method of Symmetrical Coordinates Applied to the Solution of Polyphase Networks," AIEE Transactions, Vol. 37, Part II, pp 1027-1140, 1918.

5. R. W. Hamming, Numerical Methods for Scientists and Engineers, McGraw-Hill Book Company, pp 67-78, 1962.

6. R. H. MacNeal (ed.), "The NASTRAN Theoretical Manual (Level 15)," NASA SP-221(01), April 1972.

7. "Analysis of a Solid Rocket Motor Cavity," The MacNeal-Schwendler Corporation Report MS-220, November 22, 1972.

	L and R Half-Segment Model	S and A Half-Segment Model	Dihedral Transform Model
Side 1 Even Comp	$u^{n+1,R} = u^{n,L}$	$u^{n+1,S} + u^{n+1,A} = u^{n,S} - u^{n,A}$	$u^{o,A} = -su^{kc,S} + cu^{ks,A} =$ $-su^{ks,S} - cu^{kc,A} = u^{N/2,S} = 0$
Side 1 Odd Comp	$u^{n+1,R} = -u^{n,L}$	$u^{n+1,S} + u^{n+1,A} = -u^{n,S} + u^{n,A}$	$u^{o,S} = cu^{kc,S} + su^{ks,A} =$ $cu^{ks,S} - su^{kc,A} = u^{N/2,A} = 0$
Side 2 Even Comp	$u^{n,L} = u^{n,R}$	$u^{n,A} = 0$	$\bar{u}^{o,A} = \bar{u}^{kc,A} = \bar{u}^{ks,A} = \bar{u}^{N/2,A} = 0$
Side 2 Odd Comp	$u^{n,L} = -u^{n,R}$	$u^{n,S} = 0$	$\bar{u}^{o,S} = \bar{u}^{kc,S} = \bar{u}^{ks,S} = \bar{u}^{N/2,S} = 0$

where $c = \cos k\pi/N$, $s = \sin k\pi/N$

Table 1. Boundary Compatibility Constraints for the Case of Dihedral Symmetry

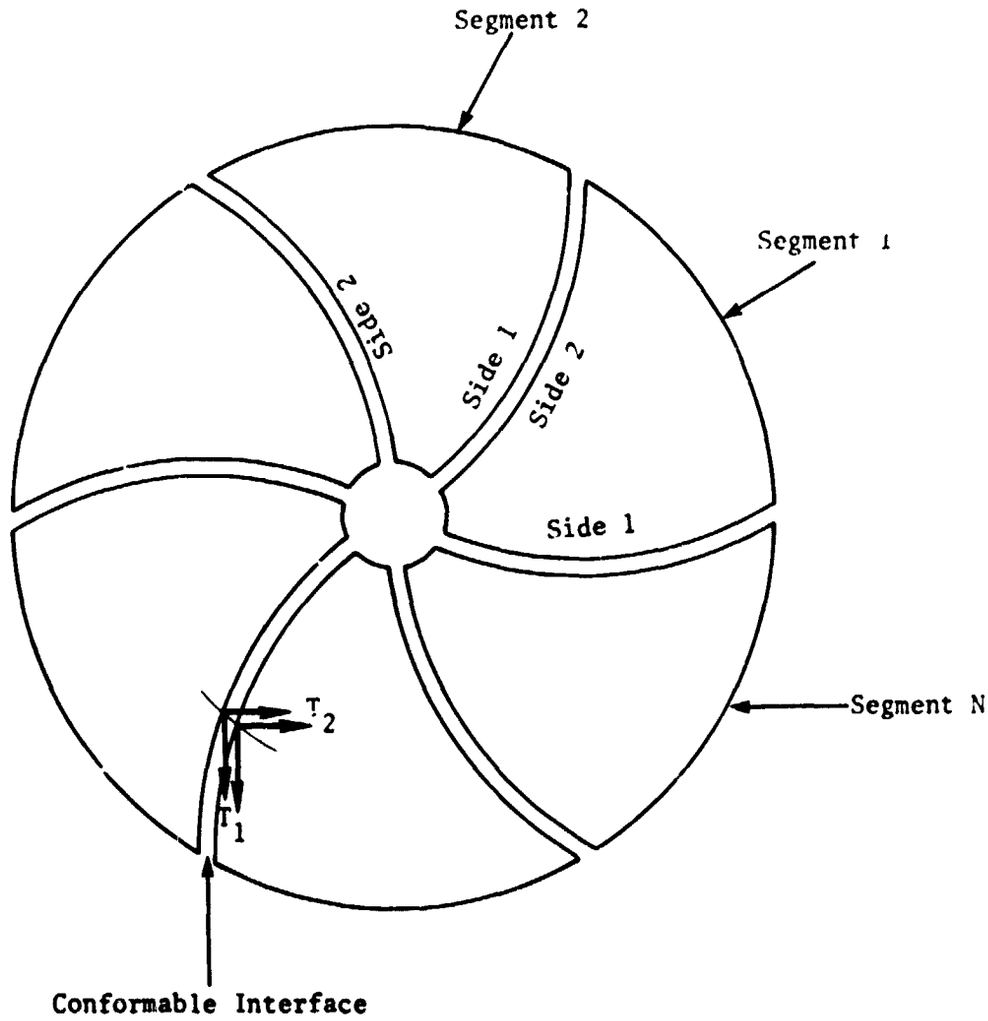

1. The user models one segment.
2. Each segment has its own coordinate system which rotates with the segment.
3. Segment boundaries may be curved surfaces. The local displacement coordinate systems must conform at the joining points. The user gives a paired list of points on Side 1 and Side 2 which are to be joined.

Figure 1. Rotational Symmetry

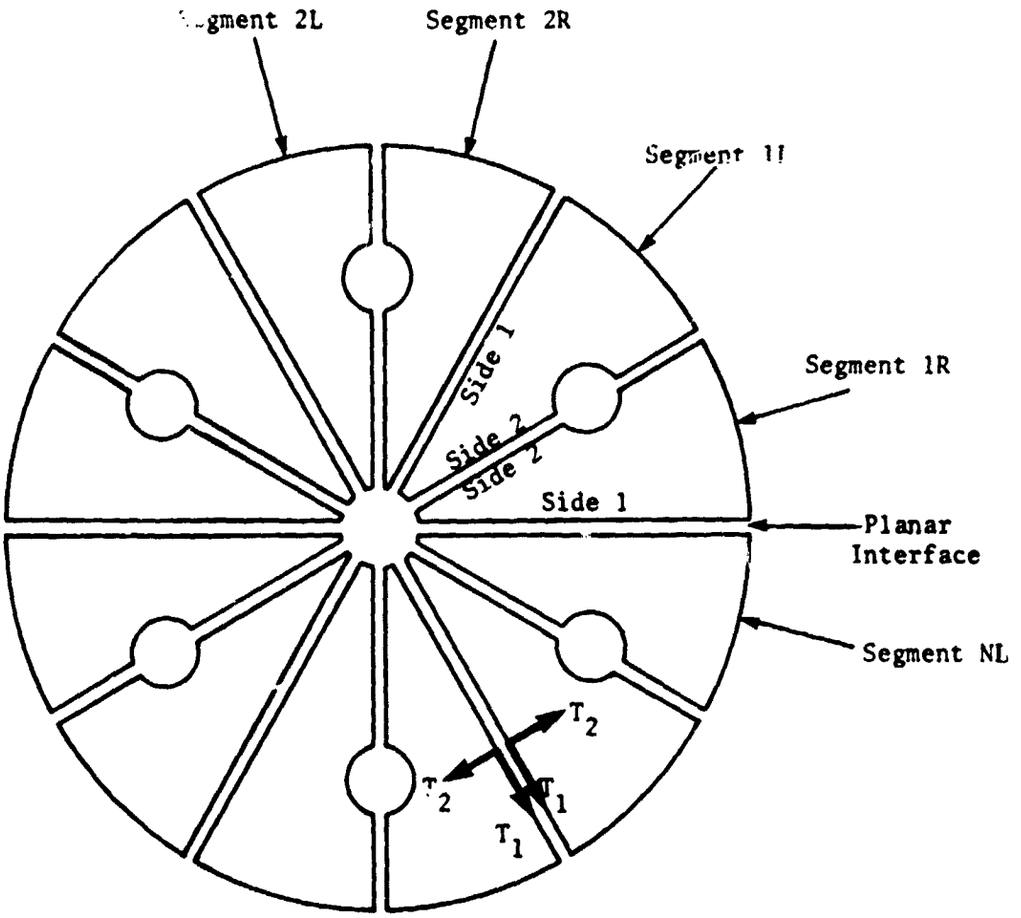

1. The user models one-half segment (an R segment). The L half segments are mirror images of the R half segments.
2. Each half segment has its own coordinate system which rotates with the segment. The L half segments use left hand coordinate systems.
3. Segment boundaries must be planar. Local displacement systems axes, associated with intersegment boundaries, must be in the plane or normal to the plane. The user lists the points on Side 1 and Side 2 which are to be joined.

Figure 2. Dihedral Symmetry

Input Data Card SPCD

Description: Defines an enforced displacement value for static analysis, which is requested as a LØAD.

Format and Example:

1	2	3	4	5	6	7	8	9	10
SPCD	SID	G	C	D	G	C	D		
SPCD	100	32	436	-2.6	5		+2.9		

Field	Contents
SID	Identification number of a static load set. (Integer > 0)
G	Grid or scalar point identification number (Integer > 0)
C	Component number (6≥ Integer ≥ 0 ; up to six unique such digits may be placed in the field with no imbedded blanks)
D	Value of enforced displacement for all coordinates designated by G and C (Real)

Remarks:

1. A coordinate referenced on this card must be referenced by an SPC or SPC1 data card.
2. Values of D will override to values specified on an SPC Bulk Data card, if the LØAD set is requested.
3. The Bulk Data LØAD combination card will *not* request an SPCD.
4. At least one Bulk Data load card (FØRCE, SLØAD, etc.) is required in the load set selected in case control.

Figure 3. SPCD Bulk Data Card Format

Input Data Card CYJØIN

Description: Defines boundary points of segments in cyclic symmetry problems.

Format and Example:

1	2	3	4	5	6	7	8	9	10
CYJØIN	SIDE	C	G1	G2	G3	G4	G5	G6	abc
CYJØIN	1		7	9	16	25	33	64	ABC
+bc	G7	G8	G9	-etc.-					
+BC	72								

Alternate Form

CYJØIN	SIDE	C	GID1	"THRU"	GID2				
CYJØIN	2	S	6	THRU	32				

Field	Contents
SIDE	Side Identification (Integer 1 or 2)
C	Coordinate System (BCD R,C or S or blank)
Gi,GIDi	Grid or scalar point identification numbers (Integer > 0)

Remarks:

1. CYJØIN Bulk Data cards are only used for cyclic symmetry problems. A parameter (CTYPE) must specify rotational or dihedral symmetry.
2. For rotational problems there must be one logical card for SIDE=1 and one for SIDE=2. The two lists specify grid points to be connected, hence both lists must have the same length.
3. For dihedral problems, side 1 refers to the boundary between segments and side 2 refers to the middle of a segment. A coordinate system must be referenced in field 3, where R = rectangular, C = cylindrical, and S = spherical. If a rectangular system is chosen, the 1 and 3 axes must lie in the boundary plane.
4. All components of displacement at boundary points are connected to adjacent segments, except those constrained by SPC, MPC, or ØMIT.

Figure 4. CYJØIN Bulk Data Card Format

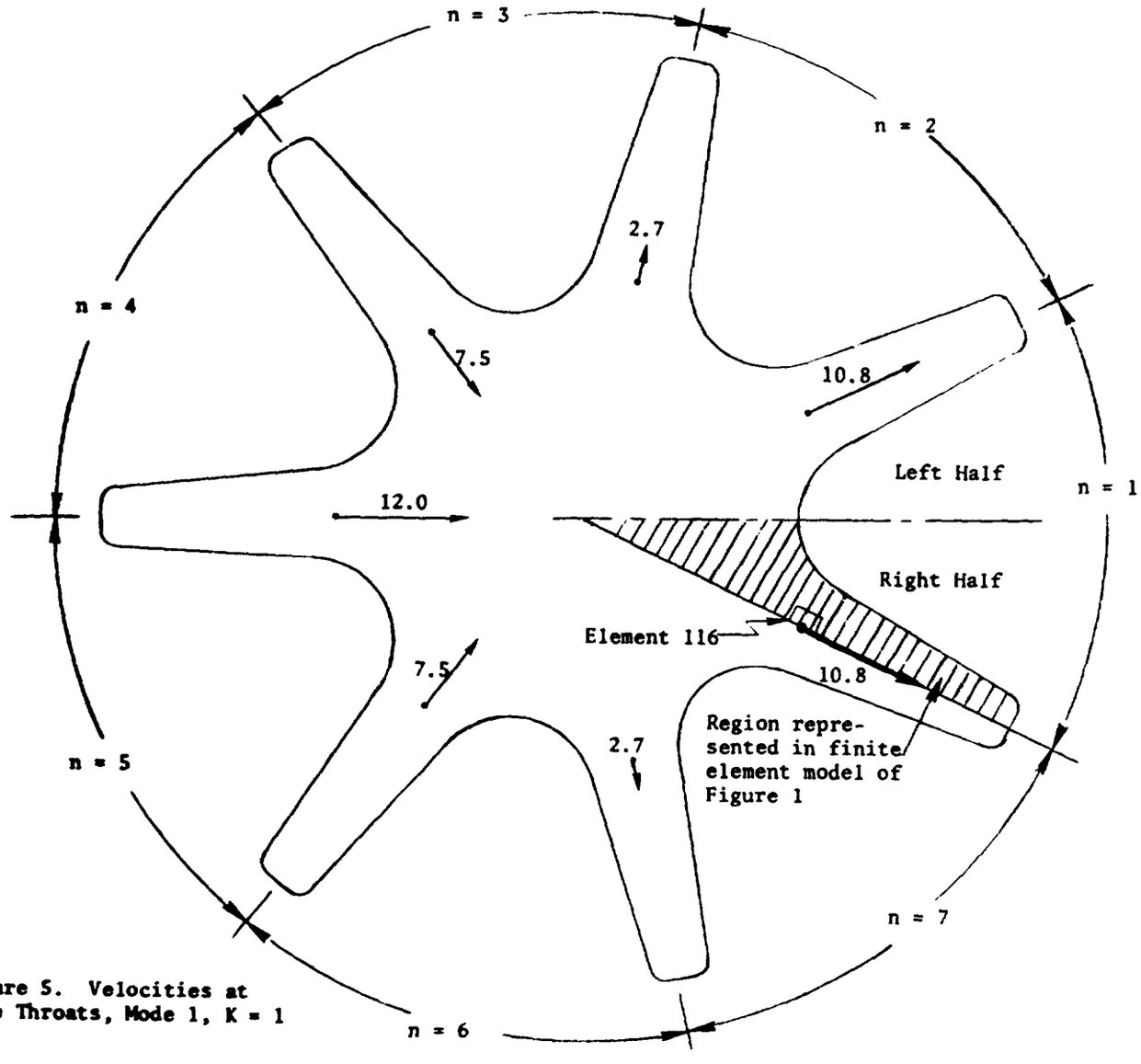

Figure 5. Velocities at Lobe Throats, Mode 1, K = 1

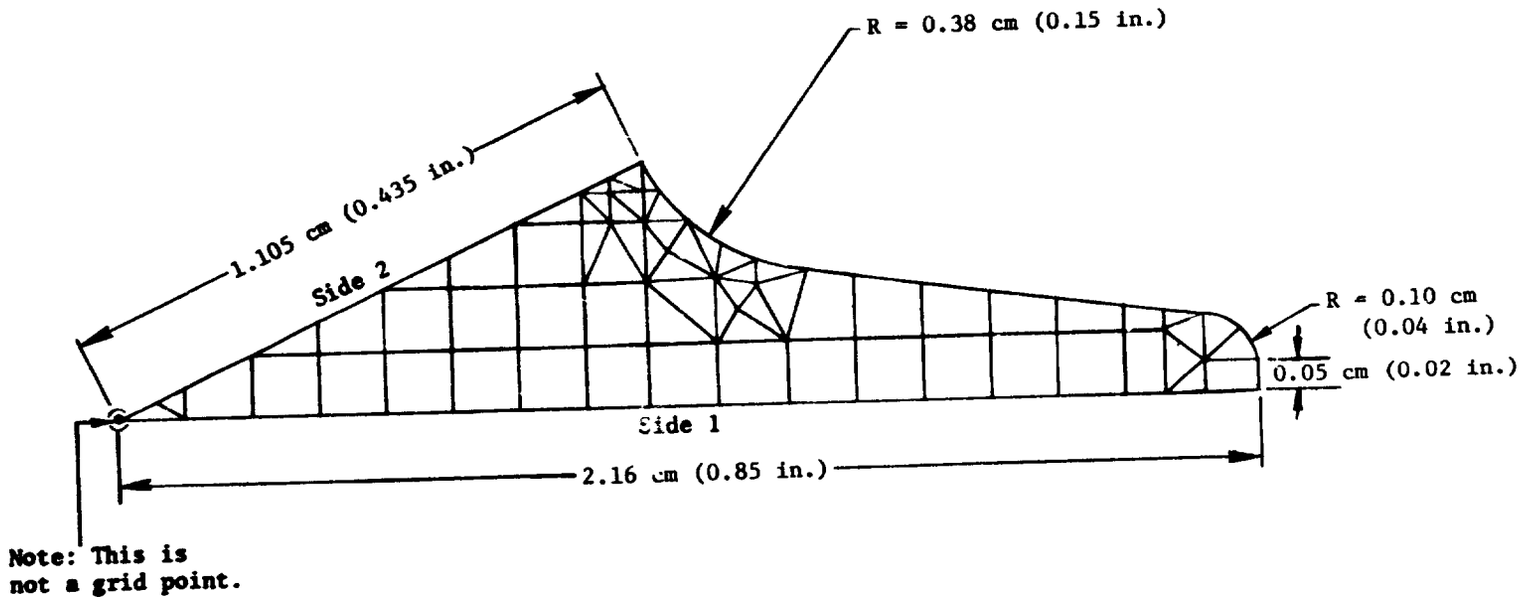

Figure 6. Finite Element Model
1/14 Sector of Cross Section

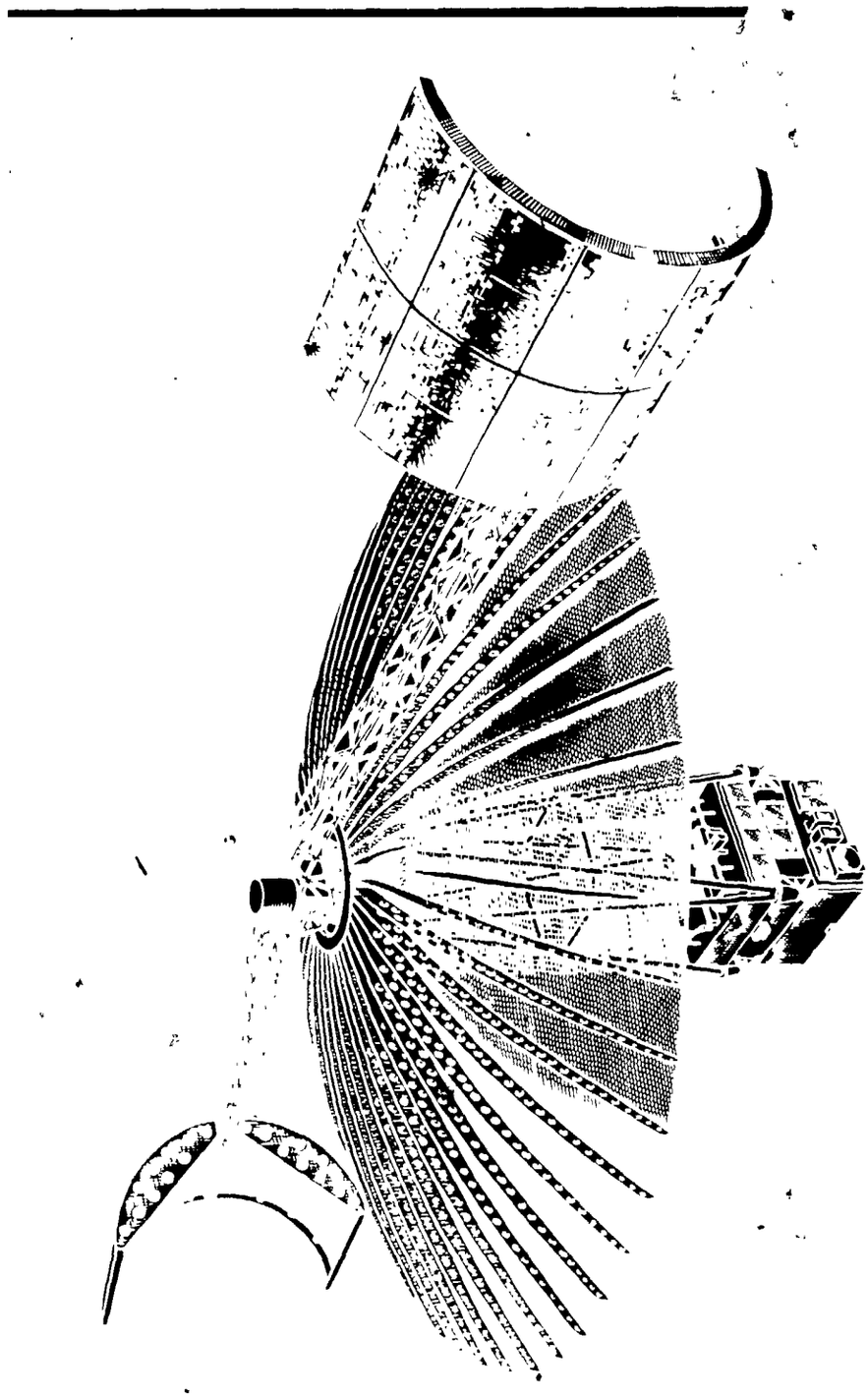

Figure 7. ATS-F Spacecraft with 30-ft Paraboloic Reflector

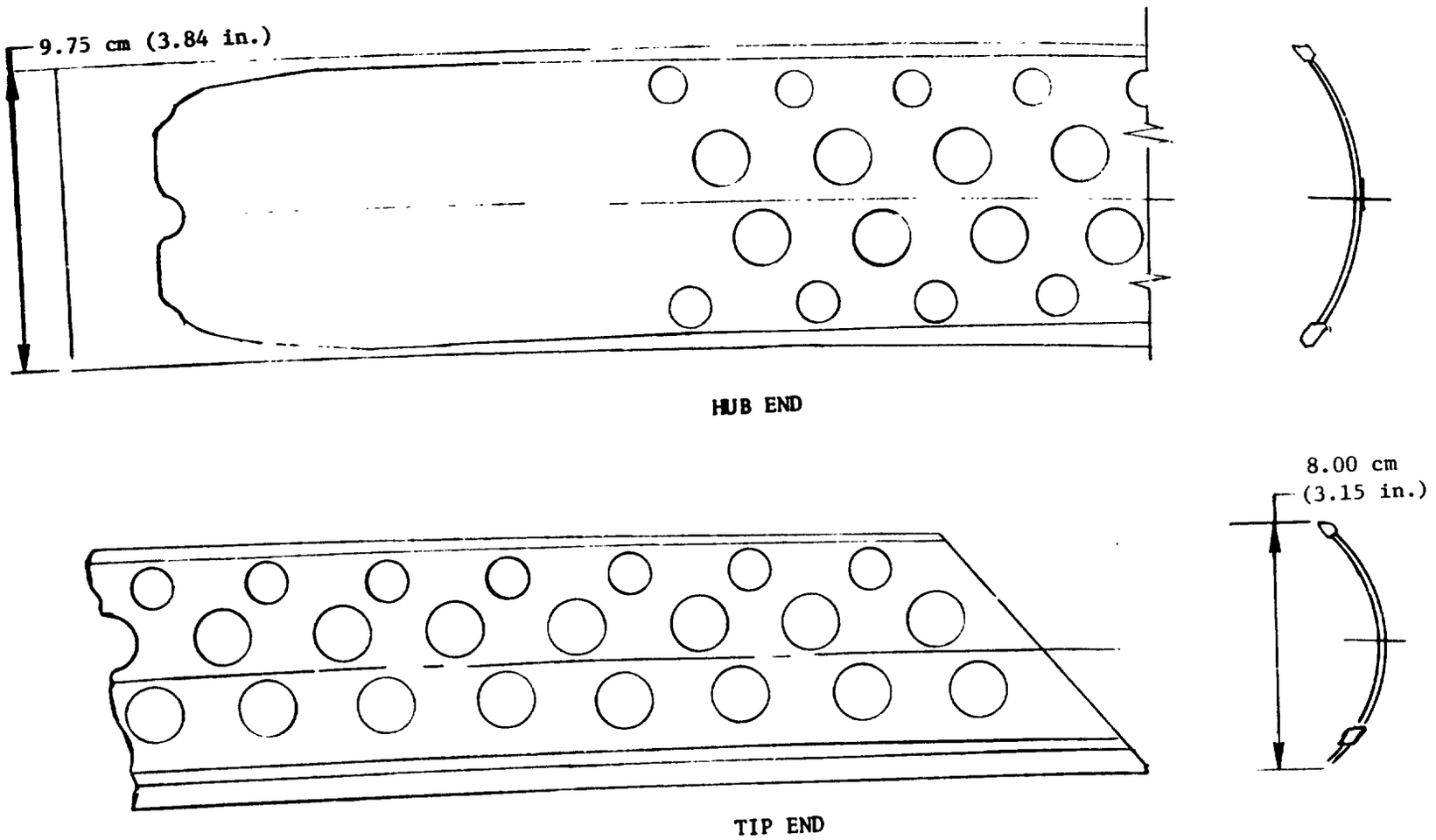

Figure 8. ATS-F Antenna Rib (Typ.)